

Short Communication

## Investigation of Corrosion Inhibition Effect of Enprofylline Drug on Mild Steel Corrosion in Sulphuric Acid Solution

Yin Liangtian<sup>1</sup>, Man Zhang<sup>2</sup>, Chen Shidong<sup>3</sup>, Tian Yunji<sup>4</sup>, Wu Haixia<sup>5,\*</sup>

<sup>1</sup> Research Institute of Oil Production Technology, The Seventh Oil Extraction Plant of Petrochina Changqing Oil Field Company, Xian, Shanxi province, China-710000.

<sup>2</sup> Research Institute of Oil Production Technology, The Fifth Oil Extraction Plant of Petrochina Changqing Oil Field Company, Xian, Shanxi province, China-710000.

<sup>3</sup> Research Institute of Oil Production Technology, The Sixth Oil Extraction Plant of Petrochina Changqing Oil Field Company, Xian, Shanxi province, China-710000.

<sup>4</sup> Research Institute of Oil Production Technology, The Tenth Oil Extraction Plant of Petrochina Changqing Oil Field Company, Xian, Shanxi province, China-710000.

<sup>5</sup> School of Chemical and Pharmaceutical Engineering, Hebei University of Science and Technology, Shijiazhuang, Hebei, China-050018.

\*E-mail: [wuhaixiawjj@163.com](mailto:wuhaixiawjj@163.com)

Received: 9 February 2020 / Accepted: 1 April 2020 / Published: 10 May 2020

---

The drug Enprofylline (DE) [3-propylxanthine] was examined as potential corrosion inhibitor of mild steel in 1 M sulphuric acid (H<sub>2</sub>SO<sub>4</sub>) media using weight loss, electrochemical, surface and quantum chemical studies. DE is basically a bronchodilator and has been used in treatment of asthma for a very long time. This drug was chosen due to its non-toxicity, ease of availability and low cost. The presence of nitrogen and oxygen (N, O) heteroatoms in the molecular structure makes it potential inhibitor for corrosion of mild steel in sulphuric acid. The electrochemical tests including open circuit potential (OCP), electrochemical impedance spectroscopy (EIS), and potentiodynamic polarization (PDP) showed good mitigation efficiency of DE in 1M H<sub>2</sub>SO<sub>4</sub> media. The variation of the anodic and cathodic slopes reflected that the DE belongs to mixed category. All the electrochemical results were close to each other vindicating the spontaneity of the tests. The surface studies were done using scanning electrochemical microscopy (SECM) and scanning electron microscopy with energy dispersive spectroscopy (SEM-EDS). Theoretical simulations were done using Gaussian 9.0 software for windows using density functional theory (DFT). The DFT simulations were done for both neutral and protonated molecules to get better idea of the mechanism of action.

---

**Keywords:** Enprofylline, Mild steel, H<sub>2</sub>SO<sub>4</sub>, Corrosion inhibition, EIS, SECM

### 1. INTRODUCTION

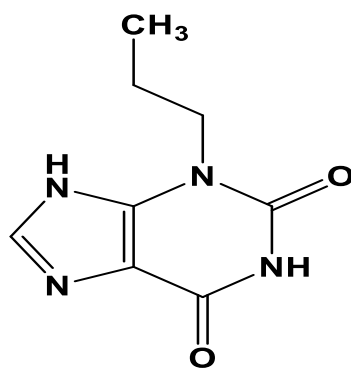
Mild steel is used worldwide due to its cost, availability and large tenders. Almost all oil and petroleum companies use mild steel due to its varied applications. Low carbon steel is an appropriate

material for the tanks to store oil, pipelines to transport oil and gas, boilers, casing and tubing pipes for oil recovery [1]. To enhance oil recovery, the tanks are washed with acid solutions including hydrochloric and sulphuric acids. Sometimes, to remove the clogging or precipitations on the internal side of transportation pipelines they are treated with acidic solutions. These acidizing solutions may cause severe corrosion in the storage tanks, pipelines or oilfield reservoir [2]. The corrosion can lead to severe accidents and fatal failures. Most of the time it is impossible to determine the internal corrosion that occurs beneath the coatings of the storage tanks or pipelines. The internal corrosion if not monitored or treated can grow exponentially throughout the tank and pipeline forming cracks and pits. These cracks and pits can further lead to fatal accidents and shutdown of the place. Therefore, the need of effective corrosion inhibitor is always in acidizing industries that can be mixed with acidic media during the treatment of the tanks and pipelines.

There are many techniques to control corrosion and use of inhibitors is one of them. It is widely used due to its ease of application, simple instruments, low cost and effectiveness. The environment and government regulations do not allow use of toxic compounds as inhibitors in high concentrations. Inhibitors are used in scaling, pickling, acidization and cleaning industries to inhibit the corrosion process. These compounds can inhibit corrosion effectively but in lower concentration may not work always depending on the surface area. In order to use inhibitors in high concentration while being non-toxic extraction of natural substances/compounds from different parts of plants (fruit, stem, leaves, and seed) was performed. Several authors received good results using these compounds from plants in acidizing and pickling industries [3-10]. The achieved results exhibited that plant extracts could function as potential corrosion inhibitors but for a short duration of time. For long time interval the plant extracts showed growth of fungus that deteriorated the inhibition efficiency. So to enhance the inhibition activity drugs were used before by several authors due to their non-toxicity and effectiveness. The drugs are rich in  $\pi$  bonds, benzene rings, conjugated double bonds, and heteroatoms (N, S, O, P) that makes them very competent. A wide class of drugs have similar structures to these carbon-based complexes including pyridines, furans, imidazoles, thiophenes, isoxazoles etc [11-20]. Being eco-friendly, and non-toxic, drugs ideally suit the environmental regulations over the toxic inhibitors. They can be used in low and high concentrations for acidization, scaling and pickling industries. Therefore, a number of research work is done using new and expired medications as corrosion inhibitors [21-25]. The outcome of using the expired drugs were surprising as they prove to be ideal and cost effective corrosion inhibitors than being a pharmaceutical compound that needs to be disposed of [26-28].

Enprofylline with propylxanthine at position 3 is a xanthine derivative used in the treatment of asthma acting as a bronchodilator. It is used in asthma, chronic obstructive pulmonary disease, in the management of cerebrovascular insufficiency, sickle cell disease, and diabetic neuropathy. Long-term usage may be associated with elevation in liver enzyme levels and unpredictable blood levels. Along with erythrocyte activity, it also decreases blood viscosity by reducing plasma fibrinogen concentrations and increasing fibrinolytic activity. Moreover, it has a role as a non-steroidal anti-inflammatory drug, a bronchodilator agent, an anti-asthmatic drug and an anti-arrhythmia drug.

Structure and IUPAC name of DE shown in Fig. 1. The present work shows the outcome of Enprofylline (DE) on the mild steel corrosion in 1M H<sub>2</sub>SO<sub>4</sub> media using the electrochemical and surface methods.



**3-propyl-3,9-dihydro-1H-purine-2,6-dione**

**Figure 1.** Structure and IUPAC name of Enprofylline (DE).

## 2. EXPERIMENTAL SECTION

The expired Enprofylline (DE) tablets were purchased from the pharmacy. It was weighed and powdered to fine particles. The powder was further solubilize in hot water and then refluxed with 1 M sulfuric acid for 5 hours at 70 °C. The solid remnants on the filter paper were weighed and discarded. The solvent was further used for corrosion inhibition experiments.

Mild steel samples of specified dimensions were used for all the tests. The mild steel samples were prepared as test electrodes embedded in epoxy resin with open 1 cm<sup>2</sup> area for electrochemical experiments. The specimens were abraded according to ASTM A262, and cleaned following the ASTM G-1 standard. The acidic solution of 1 M H<sub>2</sub>SO<sub>4</sub> was organized from analytical rated H<sub>2</sub>SO<sub>4</sub> and distilled water.

Gamry workstation was connected to the three cell assembly with mild steel (working electrode), platinum electrode (auxiliary electrode) and saturated calomel electrode (reference electrode) to carry out the electrochemical tests. All the obtained data was analyses through Echem analyst software delivered by Gamry devices. EIS measurements were conducted under static conditions from 100 kHz to 0.01 Hz, with an amplitude of 10 mV. All potentials reported were measured in the range +250 mV – 250 mV versus reference electrode. Polarization curves were carried out at a scan rate of 1.0 mVs<sup>-1</sup>. The tests were conducted when the system showed a stable open circuit potential (OCP) with and without inhibitor. The efficiency of inhibition is obtained using the equation below:

$$\eta\% = \frac{R_{ct(inh)} - R_{ct}}{R_{ct(inh)}} \times 100 \quad (1)$$

Where  $R_{ct(inh)}$  and  $R_{ct}$  be the charge transfer resistance with and without inhibitor in 1M sulfuric acid medium. The values of corrosion current density ( $I_{corr}$ ) can be used to calculate the efficiency of inhibition ( $\eta$  %) through the equation below:

$$\eta\% = \frac{I_{corr} - I_{corr(i)}}{I_{corr}} \times 100 \quad (2)$$

Where  $I_{corr}$  and  $I_{corr(i)}$  be the corrosion current density with and without inhibitor.

The scanning electrochemical microscopy (SECM) tests were performed on Chi workstation. The tests were performed to check for localized corrosion using current versus probe distance. The scanning electron microscopy (SEM) with energy dispersive spectroscopy (EDS) was done to detect the changes at the external area of the metal. SEM was conducted using Tescan machine equipped with Zeiss lens. The samples were washed with sodium bicarbonate solution to remove the corrosion products followed by distilled water prior to surface exposure.

Quantum simulations are done to support the experimental data with the theoretical parameters. Simulations were conducted using Gaussian 09 software and figures were obtained using Gauss view 5.0 software. Density function theory (DFT) method with B3LYP module was chosen for all atoms. Highest occupied molecular orbital (HOMO), Lowest unoccupied molecular orbital (LUMO), and dipole moment ( $\mu$ ) were investigated [29].

### 3. RESULTS AND DISCUSSION

#### 3.1 Electrochemical measurements

##### 3.1.1. Open Circuit Potential (OCP)

The open circuit potential was run on the electrochemical workstation with the three cell assembly wired to the workstation. This was run after an interval of 30 minutes to allow the solution and electrodes to stabilize. The test was run for 200 seconds and after 30 minutes of immersion time the potential was quite stable for all concentrations. The obtained open circuit potential was stable for blank solution (1M H<sub>2</sub>SO<sub>4</sub>) and inhibited solutions as can be seen in Fig. 2.

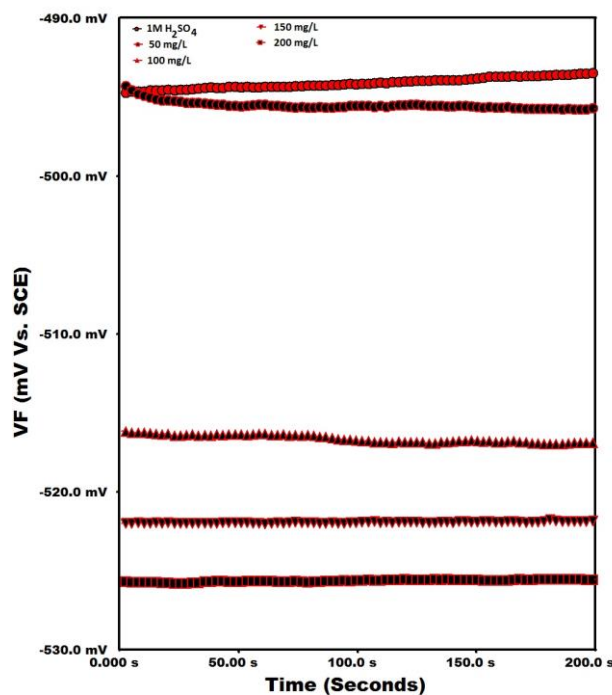


**Figure 2.** Open circuit potential plots for mild steel in 1 M H<sub>2</sub>SO<sub>4</sub> with and without DE.

3.1.2. Electrochemical impedance spectroscopy (EIS) tests

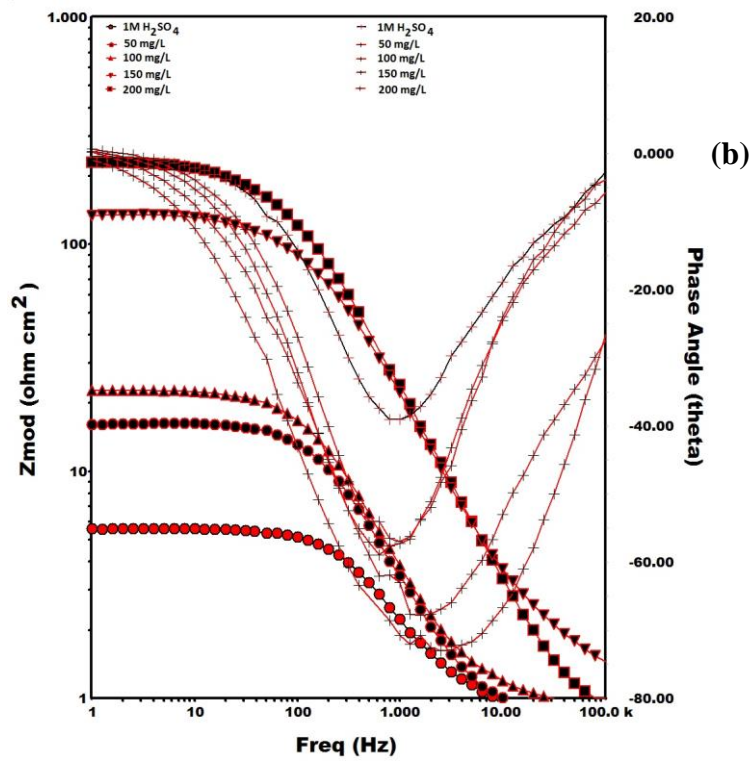
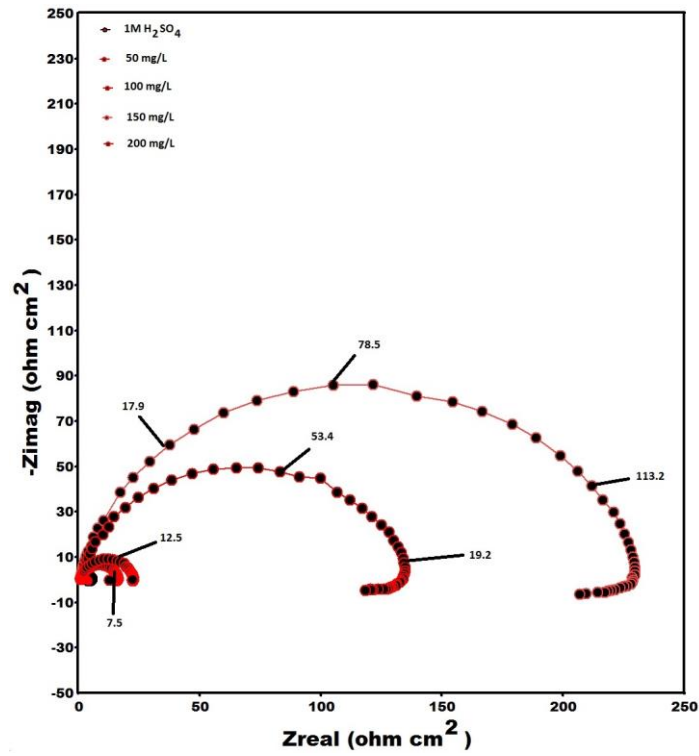
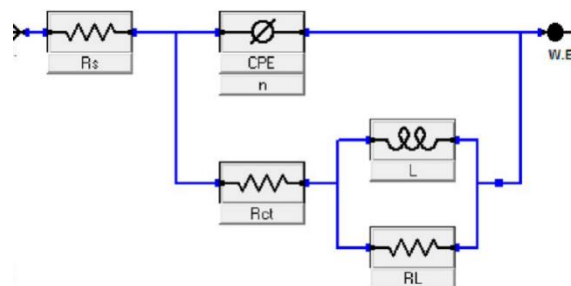


Figure 3. (a) Nyquist and (b) bode-phase angle plots for mild steel in 1 M H<sub>2</sub>SO<sub>4</sub> with and without DE.



**Figure 4.** Corresponding Randle’s circuit used to fit Nyquist plots in 1 M H<sub>2</sub>SO<sub>4</sub> with various concentrations of DE.

**Table 1.** Electrochemical impedance parameters for mild steel in 1 M H<sub>2</sub>SO<sub>4</sub> solution with and without DE

Solutions mg/L	$R_{ct}$ ( $\Omega\text{ cm}^2$ )	$n$	$Y_0$ ( $10^{-6}\Omega^{-1}\text{ cm}^{-2}$ )	$L$ %	$\eta$	Slope	Phase angle ( $\theta$ )
Blank	08	0.57	289	-	-	0.44	38
50	33	0.59	239	09	75	0.478	59
100	39	0.59	214	37	79	0.50	60
150	142	0.66	188	26	94	0.56	73
200	232	0.69	134	17	96	0.61	79

Nyquist figures of mild steel in 1 M H<sub>2</sub>SO<sub>4</sub> with and without DE are specified in Fig. 3a, and it can be detected that the width of the semicircle rises with increasing DE adsorption. This rise in semicircles of capacitance recommends that the mitigation behavior of DE is because of adsorption on the mild steel facet deprived of varying the corrosion process [43-45]. Moreover, Fig. 3a shows the higher and lower frequency regions with similar capacitance but with different diameter.

In the bode plots (Fig. 3b), the slope values tend to increase in existence of DE than in its nonexistence (Table 1). This indicates the good potential of DE on steel surface. In phase angle plots (Fig. 3b), at the intermediate frequency the dimension of the peak and phase angle parameter increases as the DE concentration increases. The highest peak at 79.4° (200 mg/L) DE concentration for mild steel was observed and reported in Table 1. This shows the development of preventive obstacle that saves the steel facet [46]. Hence, the adsorbed molecules of DE on the steel facet increases the corrosion mitigation property of steel.

The outcome of the impedance values achieved afterwards fitting the curves of Nyquist with the corresponding circuit (Fig. 4) are shown in Table 1. The Randle’s equivalent circuit model contains capacitance CPE, inductance ( $L$ ,  $R_L$ ), which is in parallel with charge transfer resistance ( $R_{ct}$ ) and they are overall in series with the solution resistance ( $R_s$ ). CPE can be used instead of pure capacitor

The frequency dependent distribution of the current density along the metal surface can be compensated by using the CPE in place of pure capacitor [47]. The subsequent equation was used to analyse the impedance (ZCPE):

$$Z_{CPE} = Y_0 [j\omega^\alpha]^{-1} \tag{3}$$

where  $j$  represents imaginary value ( $j = \sqrt{-1}$ ),  $Y_0$  represents the CPE constant,  $\omega$  be the angular frequency, and  $\alpha$  be the phase change [43]. The correlation between the  $C_{dl}$  and CPE can be measured by the equation [48]:

$$C_{dl} = Y_0^{1/\alpha} \left[ \frac{1}{R_s} + \frac{1}{R_{ct}} \right]^{(\alpha-1)/\alpha} \tag{4}$$

According to the Table 1, the  $R_{ct}$  values rises and  $C_{dl}$  declines with the add-on of the DE to the acidic media. The observed phenomenon is due to the adsorption of DE fragments on the mild steel facet and reduces the straight connection between the metal and hostile media [49]. Also, the better efficiency of inhibition in existence of DE support the wide covering quality.

### 3.1.3. Polarization tests

Fig. 5 depicts the potentiodynamic polarization pictures of the mild steel with and without DE in 1 M  $H_2SO_4$  media. As can be observed from the figure that both the hydrogen evolution (cathodic) and steel dissolution (anodic) processes were affected after the accumulation of DE in the acidic solution [50]. Although, the overall mechanism was not affected by the addition of the DE as neither the anodic nor the cathodic shift was observed.

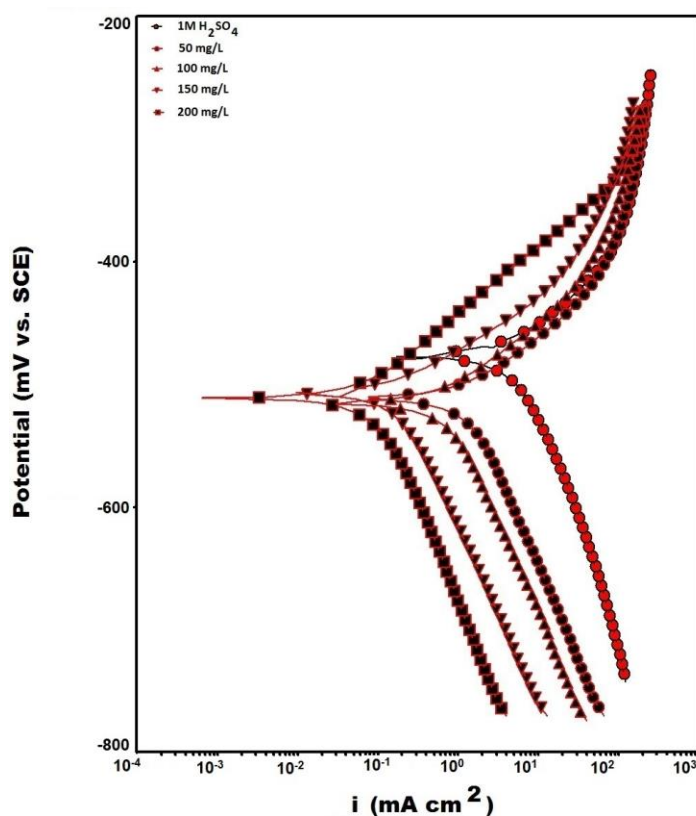


**Figure 5.** Polarization curvatures for mild steel in 1 M  $H_2SO_4$  in presence of different concentrations of DE.

The little shift towards cathodic region after the addition of DE, may be owing to the fact that the adsorption of DE molecules on the steel surface hindered the corrosive media attack on the working electrode as is evident from the  $-\beta_c$  values reported in Table 2 [51]. So, the addition of DE in the acidic solution did not changed the overall corrosion mechanism. There was also a little change in the anodic values of  $\beta_a$  that may be endorsed to the development of protective layer of DE molecules on the mild steel surface that further blocked the active centers present on the surface, thereby slowing the dissolution process [52].

**Table 2.** Electrochemical polarization parameters for mild steel in 1 M H<sub>2</sub>SO<sub>4</sub> solution with and without DE.

DE (mg/L)	$E_{\text{corr}}$ (mV/SCE)	$I_{\text{corr}}$ ( $\mu\text{A cm}^{-2}$ )	$\beta_a$ (mV dec <sup>-1</sup> )	$-\beta_c$ (mV dec <sup>-1</sup> )	$\eta_p$ (%)
1 M H <sub>2</sub> SO <sub>4</sub>	-477	342	54	118	–
50	-507	152	58	181	56
100	-511	76	76	113	78
150	-512	16	37	90	95
200	-515	09	61	72	97

The maximum inhibition efficiency of 97% at 200 mg/L concentration was observed suggesting the lower corrosion rate in presence of DE. The corrosion potential did not showed much variation or shift and was quite stable. The conclusions of research papers suggests that if the shift or movement in corrosion potential is  $\geq 85$  mV with reference to the blank (1M H<sub>2</sub>SO<sub>4</sub>) solution, then only DE can be classified into anodic or cathodic inhibitor [53]. But, from Fig. 5 and Table 2, the shift is very evident and is found to be 38 mV. So, based on this theory DE can be classified as mixed type inhibitor.

### 3.2 Surface Characterization

#### 3.2.1. SECM

The electrochemical information about the localized corrosion taking place at the metal surface can be determined using SECM. This technique has proved to be very useful in recent years due to its accuracy and very helpful in predicting corrosion mechanisms. One of the benefit of using SECM is that it can incorporate both insulating (coated / films) and conducting (non-coated) surfaces. This can help in comparison of both the surfaces in different mediums and can help to derive a suitable mechanism of action [40].

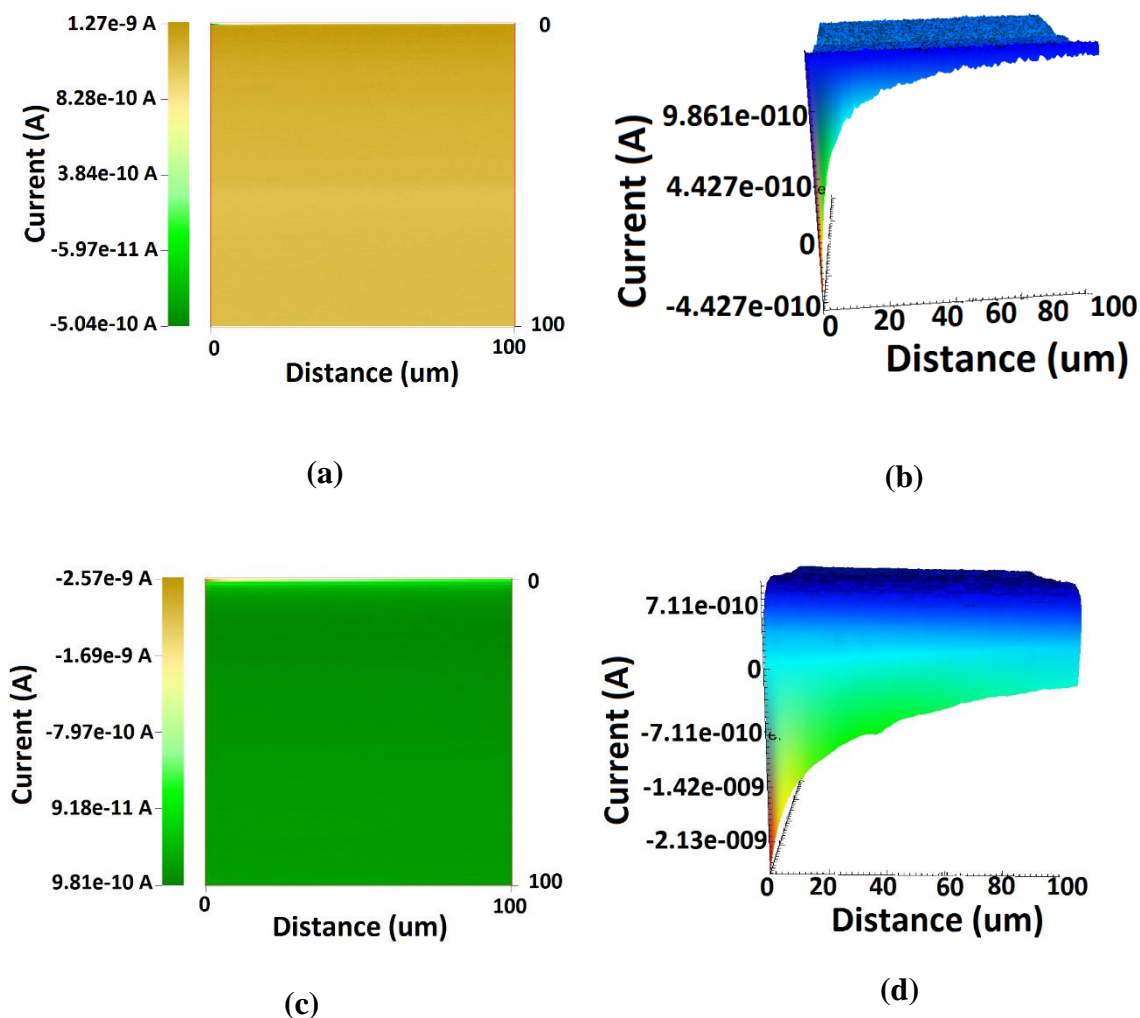


**Figure 6.** SECM images for mild steel (a) 2D graph for 1M H<sub>2</sub>SO<sub>4</sub> (b) 3D graph for 1M H<sub>2</sub>SO<sub>4</sub> (c) 2D graph for 200 mg/L DE and (d) 3D graph for 200 mg/L DE.

A probe approach curve is done before the start of each test to establish the same distance for each exposed samples. As the tip aligns the metal surface the changes in current of the system can be observed [41]. All the metal samples were submerged in the corrosive medium for 20 minutes before the start of tests. The 2D and 3D images of SECM test for mild steel in 1M H<sub>2</sub>SO<sub>4</sub> with and without DE is shown in Fig. 6. As the probe tip comes near the steel surface without inhibitor, rise in current is perceived due to the conducting behavior of steel. Here, as the tip is in straight contact with the metal surface, the conducting activity is observed vindicated by the increase in current on x axis as shown in Fig. 6a, 6b. On the other hand, when the probe comes near the metal surface with DE inhibitor the current is reduced as the metal begins to act as insulating surface. This is due to the existence of DE inhibitor film on the steel surface in 1M H<sub>2</sub>SO<sub>4</sub> medium that forms a protective layer and inhibits the corrosive solution on x axis as displayed in Fig. 6c, 6d. After the comparison of currents for mild steel samples with DE inhibitor and samples without DE inhibitor, the effective corrosion inhibition of DE molecules for steel in H<sub>2</sub>SO<sub>4</sub> medium can be confirmed.

### 3.2.2 SEM characterization

To observe the range of protection of the steel surface by DE, the morphology of mild steel surface submerged in 1M H<sub>2</sub>SO<sub>4</sub> without and with 200 mg/L DE was checked using SEM. In order to get a clear picture of DE action the steel surface without DE was exposed to SEM first and the result is represented in Fig. 7a. The surface is very rough, corroded and irregular. The corrosive solution attacked the mild steel surface and due to oxidation the steel formed rust after corroding. While, in presence of DE the steel surface was smooth, regular and less corroded as shown in Fig. 7b. The abraded lines can be seen and the surface is much better than without DE. This proposes that the DE formed a shielding layer on the steel surface that inhibited the corrosion progression by blocking the corrosive solution from attacking the metal surface.

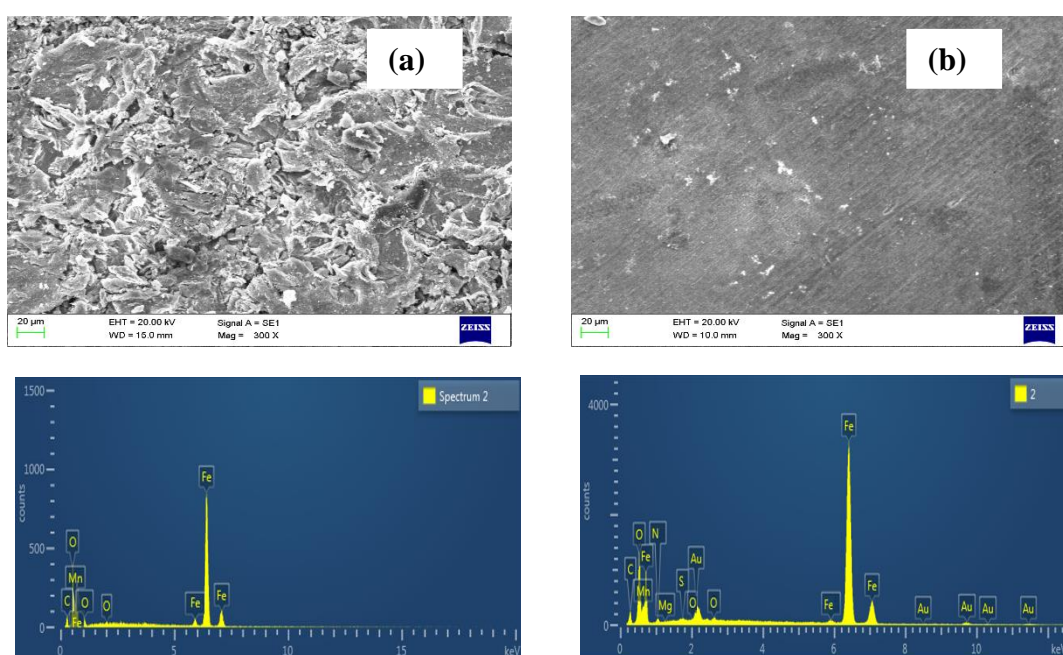


**Figure 7.** SEM-EDS images for mild steel (a) 1 M H<sub>2</sub>SO<sub>4</sub>, and (b) 200 mg/L DE.

### 3.3. Quantum Chemical Investigations

The simulations were run to find the optimized geometry for the inhibitor. After the optimized geometry was obtained further studies were performed to get the detailed content about the molecular orbitals. The obtained computational structures are displayed in Fig. 8. Fig. 8a, 8b, 8c shows the optimized geometry, highest occupied molecular orbital (HOMO) and the lowest unoccupied molecular orbital (LUMO) structures of neutral DE molecule. Fig. 8d, 8e, 8f shows the optimized geometry, highest occupied molecular orbital (HOMO) and the lowest unoccupied molecular orbital (LUMO) structures of protonated DE molecule. Likewise, the obtained parameters including  $E_{\text{HOMO}}$ ,  $E_{\text{LUMO}}$ ,  $\Delta E$  (LUMO-HOMO), dipole moments ( $\mu$ ) are enumerated in Table 3. HOMO and LUMO represents the active sites through which the nucleophilic and electrophilic substitution reactions takes place. In other words, these

sites provide the information about the electron donor and electron acceptor atoms in the inhibitor molecule.

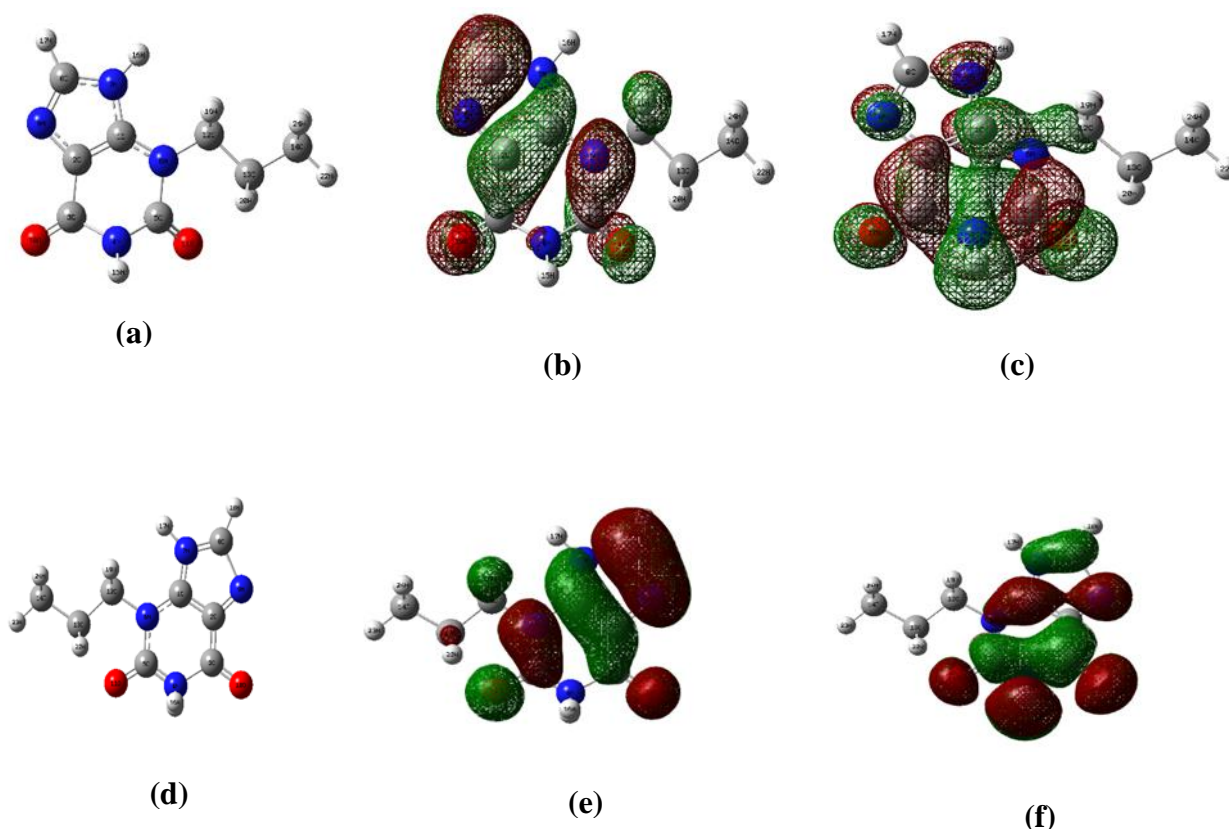


**Figure 13.** (a) Optimized molecular structure of neutral DE (b) Optimized molecular structure of protonated DE, (c) HOMO of neutral DE (d) HOMO of protonated DE (e) LUMO of neutral DE (f) LUMO of protonated DE.

The computational studies indicate towards the HOMO values that shows the electron donating tendency to the molecules ready to accept with vacant and low energy orbital. Meanwhile, the LUMO values indicate the inclination to accept electrons being the lower unoccupied orbitals [54]. The reactivity of the DE molecules towards the steel surface is represented by the energy gap  $\Delta E$  that serves to be an important parameter. The computational calculations also confirm the relocation of electrons from the DE molecules to the steel facet leading to the bond formation that inhibits corrosion [55].

**Table 3.** Computational parameters of DE Inhibitor using Gaussian 09 software.

Quantum Parameters	Neutral DE	Protonated DE
HOMO (eV)	-5.695	-10.043
LUMO (eV)	-0.959	-6.676
$\Delta E$ (eV)	4.736	3.367
Dipole Moment ( $\mu$ )	7.5888	2.2269

#### 4. CONCLUSIONS

- Enprofylline drug can be used as potential corrosion inhibitor for mild steel in 1M H<sub>2</sub>SO<sub>4</sub> solution.
- The impedance studies showed that the charge transfer resistance increases in presence of DE.
- Polarization studies pointed that the anodic and cathodic shifts are mixed type in nature, so the DE could be categorized in mixed class inhibitor.
- SEM showed the smooth mild steel surface with less roughness in presence of DE.

#### ACKNOWLEDGMENT

Authors are thankful to all the funding agencies for their support.

#### References

1. Aijuan Zhao, H. Sun, L. Chen, Y. Huang, X. Lu, B. Mu, H. Gao, S. Wang, A. Singh, *Int. J. Electrochem. Sci.*, 14 (2019) 6814.
2. R. Wang, S. Luo, *Corros. Sci.*, 68 (2013) 119.
3. M. A. Bedair, M. M. B. El-Sabbah, A. S. Fouda, M. Elaryian, *Corros. Sci.*, 128 (2017) 45.
4. K.C. Emregul, A. Abbas Aksut, *Corros. Sci.*, 42 (2008) 2051.
5. M.M. Solomon, S.A. Umoren, I.I. Udoso, A.P. Udoh, *Corros. Sci.*, 52 (2010) 1317.
6. L. Zhou, Y. L. Lv, Y. X. Hu, J. H. Zhao, X. Xia, X. Li, *J. Mol. Liq.*, 249 (2018) 179.
7. A. A. Olajire, *J. Mol. Liq.*, 248 (2017) 775.
8. Ambrish Singh, K. R. Ansari, M. A. Quraishi, Hassane Lgaz and Yuanhua Lin, *J. Alloys Comp.*, 762 (2018) 347.
9. A. Singh, I. Ahamad, M. A. Quraishi, *Arab. J. Chem.*, 9 (2016) S1584.
10. A. Yousefi, S. Javadian, N. Dalir, J. Kakemam, J. Akbari, *RSC Adv.*, 5 (2015) 11697.
11. K. Azzaoui, E. Mejdoubi, S. Jodeh, A. Lamhamdi, E. Rodriguez-Castellón, M. Algarra, A. Zarrouk, A. Errich, R. Salghi, H. Lgaz, *Corros. Sci.*, 129 (2017) 70.
12. Pandian Bothi Raja, Ahmad Kaleem Qureshi, Afidah Abdul Rahim, Hasnah Osman, Khalijah Awang, *Corros. Sci.*, 69 (2013) 292-301.
13. A. A. Khadom, A. N. Abd, N. A. Ahmed, *South Afri. J. Chem. Eng.*, 25 (2018) 13.
14. E. B. Ituen, O. Akaranta, S. A. Umoren, *J. Mol. Liq.*, 246 (2017) 112.
15. M. M. Askari, S. G. Aliofkhazraei, A. Hajizadeh, *J. Nat. Gas Sci. Eng.*, 58 (2018) 92.
16. A. Singh, Y. Lin, W. Liu, D. Kuanhai, J. Pan, B. Huang, C. Ren, D. Zeng, *J. Tai. Inst. Chem. E.*, 45 (2014) 1918.
17. A. Singh, Y. Lin, M. A. Quraishi, O. L. Olasunkanmi, O. E. Fayemi, Y. Sasikumar, B. Ramaganthan, I. Bahadur, I. B. Obot, A. S. Adekunle, M. M. Kabanda, E. E. Ebenso, *Molecules*, (2015) 2015122.
18. E.B. Ituen, M.M. Solomon, S.A. Umoren, O. Akaranta, *J. Pet. Sci. Eng.*, 174 (2019) 984.
19. D.D. Macdonald, S. Real, M. Urquidi-Macdonald, *J. Electrochem. Soc.*, 135 (1988) 2397.
20. D. Chu, R.F. Savinel, *Electrochim. Acta*, 36 (1991) 1631.
21. A.M. Abdel-Gaber, E. Khamis, H. Abo-ElDahab, Sh. Adeel, *Mater. Chem. Phys.*, 109 (2008) 297.
22. S.S. Zhang, T.R. Jow, *J. Power Source*, 109 (2002) 458.
23. A.A. El Hosary, R.M. Saleh, A.M. Shams El Din, *Corros. Sci.*, 12 (1972) 897.
24. M.A. Quraishi, A. Singh, V.K. Singh, D.K. Yadav, A.K. Singh, *Mater. Chem. Phys.*, 122 (2010) 114.
25. A. Singh, I. Ahamad, V.K. Singh, M.A. Quraishi, *J. Sol. State Electrochem.*, 15 (2011) 1087.
26. G. Gunasekaran, L.R. Chauhan, *Electrochim. Acta*, 49 (2004) 4387.

27. Ambrish Singh, K.R. Ansari, Jiyaul Haque, Parul Dohare, Hassane Lgaz, Rachid Salghi, M.A. Quraishi, *J. Taiwan Inst. Chem. E.*, 82 (2018) 233.
28. A.Y. El-Etre, M. Abdallah, Z.E. El-Tantawy, *Corros. Sci.*, 47 (2005) 385.
29. C. Verma, M.A. Quraishi, A. Singh, *J. Taibah Univ. Sci.*, 10 (2016) 718.
30. E.E. Oguzie, *Corros. Sci.*, 49 (2007) 1527.
31. R.T. Loto, *Results Phys.*, 8 (2018) 172.
32. A. Singh, E. E. Ebenso, M. A. Quraishi, Y. Lin, *Int. J. Electrochem. Sci.*, 9 (2014) 7495.
33. Dileep Kumar Yadav, M. A. Quraishi, B. Maiti, *Corros. Sci.*, 55 (2012) 254.
34. Z. Tao, S. Zhang, W. Li, B. Hou, *Ind. Eng. Chem. Res.*, 50 (2011) 6082.
35. E.S. Ferreira, C. Giacomelli, F.C. Giacomelli, A. Spinelli, *Mater. Chem. Phys.*, 83 (2004) 129.
36. D.D. Macdonald, *Electrochim. Acta*, 35 (1990) 1509.
37. K.-K. Lee, K.-B. Kim, *Corros. Sci.* 43 (2001) 561.
38. A. Singh, K.R. Ansari, A. Kumar, W. Liu, C. Songsong, Y. Lin, *J. Alloys Comp.*, 712 (2017) 121.
39. T. Rabizadeh, S. Asl, *J. Mol. Liq.*, 276 (2018) 694.
40. E. Khamis, *Corrosion* 46 (1990) 476.
41. S. Pareek, D. Jain, S. Hussain, A. Biswas, R. Shrivastava, S. K. Parida, H. K. Kisan, H. Lgaz, I. M. Chung, D. Behera, *Chem. Eng. J.*, 358 (2019) 725.
42. P. M. Krishnegowda, V. T. Venkatesha, P. K. M. Krishnegowda, S. B. Shivayogiraju, *Ind. Eng. Chem. Res.*, 52 (2013) 722.
43. A. Singh, N. Soni, Y. Deyuan, A. Kumar, *Res. Phys.*, 13 (2019) 102116.
44. X. Xu, A. Singh, Z. Sun, K. R. Ansari, Y. Lin, *R. Soc. Open Sci.*, 4 (2017) 170933.
45. P. Singh, A. Singh, M.A. Quraishi, *J. Taiwan Inst. Chem. E.*, 60 (2016) 588.
46. Y. Lin, A. Singh, E. E. Ebenso, Y. Wu, C. Zhu, H. Zhu, *J. Taiwan Inst. Chem. E.*, 46 (2015) 214.
47. I. Ahamad, R. Prasad, M. A. Quraishi, *Corros. Sci.*, 52 (2010) 933.
48. A. Singh, Y. Lin, I. B. Obot, E. E. Ebenso, *J. Mol. Liq.*, 219 (2016) 865.
49. A. Kahyarian, A. Schumaker, B. Brown, S. Nesic, *Electrochim. Acta*, 258 (2017) 639.
50. P. E. Alvarez, M. V. Fiori-Bimbi, A. Neske, S. A. Brandán, C. A. Gervasi, *J. Indus. Eng. Chem.*, 58 (2018) 92.
51. H. Feng, A. Singh, Y. Wu, Y. Lin, *New J. Chem.*, 42 (2018) 11404.
52. N. Li, S. Tang, Y. Rao, J. Qi, Q. Zhang, D. Yuan, *Electrochim. Acta*, 298 (2019) 59.
53. X. Wang, Z. Peng, S. Zhong, *Int. J. Electrochem. Sci.*, 13 (2018) 8970.
54. Yang Yaocheng, Y. Caihong, A. Singh, Y. Lin, *New J. Chem.* 43 (2019) 16058.
55. Ambrish Singh, K. R. Ansari, M. A. Quraishi, Savas Kaya, Priyabrata Banerjee, *New J. Chem.*, 43 (2019) 6303.